04,08

# *In situ* investigation of filament growth in films of stabilized zirconium dioxide by contact capacitance atomic force microscopy

© D.O. Filatov, E.D. Sorochkina, D.A. Antonov, I.N. Antonov, O.N. Gorshkov

Lobachevsky State University,
Nizhny Novgorod, Russia

E-mail: dmitry_filatov@inbox.ru

*Received May 21, 2025*
*Revised June 25, 2025*
*Accepted July 7, 2025*

The contact capacitance atomic force microscopy method was used to study processes of electroforming and resistive switching in a thin film of yttrium-stabilized zirconium dioxide on a conducting substrate. During linear voltage sweep between a probe and the substrate, there was non-linear increase of probe-sample capacitance related to formation of cluster that consisted of oxygen vacancies (a conducting filament) in the dielectric layer under the probe. With subsequent cyclic switching by sawtooth voltage, there was cyclic increase and decrease of probe-sample capacitance, which was related to respective changes of filament sizes under effect of an electric field between the probe and the substrate. Results of the present study demonstrate capabilities of the contact capacitance microscopy method for studying filament dynamics during resistive switching in the oxide films.

**Keywords:** memristor, resistive switching, filament, contact capacitance atomic force microscopy, stabilized zirconium dioxide.

DOI: 10.61011/PSS.2025.08.62256.137-25

## 1. Introduction

The memristor is a solid-state microelectronic device based on a capacitor structure, whose insulating layer can vary resistance under effect of voltage $U$ applied to plates and preserve a resistive state after deenergizing [1]. The memristors are considered to be promising for application in nonvolatile computer memory devices [2], neuromorphic computing devices [3], etc. The principle of operation of the most types of the memristors developed by now is based on formation and rupture of conducting cords (filaments) in the insulating layer in the electric field between electrodes of the memristor structure [4]. In the memristors based on metal oxides the filaments consist of the oxygen vacancies [5], while in the memristors of the „conducting bridge“ type (CB) they consist of metal atoms that are injected into an insulator from metal electrodes during anode oxidation [6].

Up to now, processes of growth of the conducting filaments in the memristors were visualized *in situ* by using a high-resolution transmission electron microscopy (TEM) method [7] as well as scanning probe microscopy (SPM) methods: scanning tunneling microscopy (STM) and atomic force microscopy (AFM) with measuring amperage of electric current through an AFM probe [8]. It is quite difficult to prepare samples for such studies. But these studies are unique and by now there is a very limited number of studies on the said topic in the literature.

The contact capacitance AFM method [10] was used in the study [9] to investigate *in situ* growth of filaments in films of yttrium-stabilized zirconium dioxide (SZD) $ZrO_2(Y)$ on the Si substrate with a Ni sublayer. It was found that capacitance $C$ between the AFM probe and the Ni sublayer was increased when applying voltage $U$ between them, which was related to formation and growth of a filament of Ni atoms in the SZD film. But the most memristors developed by now are based on metal oxide films, in which the conducting filaments consist of the oxygen vacancies. At the same time, the conducting filaments in the SV-type memristors are characterized by metal conductivity, whereas electron transport via the vacancy filaments in the oxide memristors occurs, as a rule, as per a hopping mechanism [11]. In this regard, it is of considerable interest to experimentally investigate applicability of the contact capacitance AFM method for *in situ* investigation of dynamics of the filaments in the oxide films.

The contact capacitance AFM method was applied in the present study to investigate formation and growth of vacancy filaments in the SZD/Pt films.

## 2. Materials and methods

The objects of research were thin-film SZD/Pt structures on the standard substrates Si(001), on which the insulating $SiO_2$ layers of the thickness of $\sim 500$ nm, the adhesion Ti layers and the conducting TiN layers of the thickness of $\sim 25$ nm each were preliminarily formed. The thin-film structures were formed using a vacuum installation Torr International 2G1-1G2-EB4-TH1. The SZD layer (12 mol.% of stabilizing oxide $Y_2O_3$) of the nominal thickness of $\sim 10$ nm was formed by high-frequency magnetron deposition, while the Pt layer of the thickness of $\sim 40$ nm was formed by direct-current magnetron deposition.

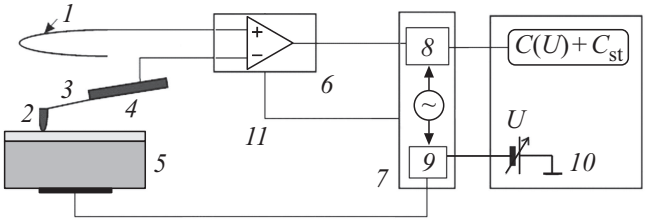


**Figure 1.** Block-diagram of measurement of capacitance between the AFM probe and the sample in the contact capacitance AFM mode. *1* — the compensatory electrode; *2* — the AFM probe, *3* — the cantilever; *4* — the base of the AFM probe; *5* — the sample; *6* — the measuring insert of the AFM head; *7* — the remote module; *8* — the synchronous detector; *9* — the summator; *10* — the AFM controller; *11* — the circuit of control of an electrical parasitic capacitance compensator (adapted from the study [12] under permission of © NT-MDT).

The contact capacitance AFM method was used to measure in the AFM „Solver Pro“ manufactured by NT-MDT in the atmospheric conditions at the room temperature by means of a special add-on device AU030 produced by NT-MDT for the contact capacitance AFM [12], which had two-step system of compensation of parasitic capacitance between the sample and other (except for the AFM probe) parts of the AFM installation (Figure 1).

1) Electromechanical compensation: a half-ring compensation electrode is placed above a cantilever beam and (partially) a base of the AFM probe; the AFM beam and the compensation electrode are connected to inputs of a differential amplifier.

2) Electrical compensation: the compensation electrode is connected to common earthing via a varicap.

Capacitance between the AFM probe and the sample is measured by applying high-frequency variable voltage of the frequency of 10 MHz between them. The output signal of the differential amplifier is supplied to a synchronous detector. The signal at the output of the synchronous detector is proportional to the magnitude $C + C_{\text{st}}$, where $C$ — capacitance between a point of the AFM probe and the sample, $C_{\text{st}}$ — incompletely compensated parasite capacitance between the sample and the other AFM parts. Special AFM probes CSG-01 produced by NT-MDT and provided with the Pt coating were used for contact capacitance AFM (a probe point curvature radius is $R_p \sim 35$ nm as specified by the manufacturer).

The experiment included measurement of capacitance $C$ between the AFM probe and the Pt sublayer during filament formation (electroforming) and cyclic switching of a virtual memristor that is formed by contact of the AFM probe point with the SZD film on the Pt sublayer with linear (sawtooth) sweep of a (quasi)-constant component of voltage between the AFM probe and the Pt sublayer $U$. The sweep amplitude was from 1 to 5 V, and its period was from 1 to 10 s. Besides, maps of capacitance distribution between the AFM probe and the Pt sublayer were recorded along the sample surface $C(x, y)$ ($x, y$ are coordinates of the AFM probe within a sample surface plane). The said measurements were carried out by means of the AFM probe DCP-30 manufactured by NT-MDT and provided with a wear-resistant conducting diamond-like coating ($R_p \sim 100$ nm).

## 3. Results and discussion

It was found that capacitance of the contact of the AFM probe with the surface of the SZD/Pt film $C$ increased during linear sweep of $U$ from 0 V to 5 V (Figure 2) due to drift of the oxygen vacancies in SZD towards the AFM probe and formation of the filament in the depth of the SZD film (the electroforming process, Figure 3). Surge-like increase of $C$ at the end of the voltage sweep process is related to growth of the filament across the entire thickness of the SZD film up to the Pt sublayer and closing of the electric circuit the AFM probe — the filament — the Pt layer.

The experimental curve of Figure 2 was interpreted using a one-dimensional model of the memristor [13]. Let us consider formation of the conducting filament of the oxygen vacancies under the contact of the Pt-coated AFM probe with the surface of the SZD/Pt film of the thickness of $d$. We assume that the filament is a cylinder with a base area $S$ and a length $\ell$.

The filament growth rate $d\ell/dt$, where $t$ is the time, can be expressed via a flow of the oxygen vacancies that penetrate through a surface of the cylinder base per unit time.

$$\frac{d\ell}{dt} = \frac{n_0}{n} v_{dr} = \frac{n_0}{n} \mu F, \tag{1}$$

where $n$ and $n_0$ — values of concentration of the oxygen vacancies in the filament volume and the SZD film,

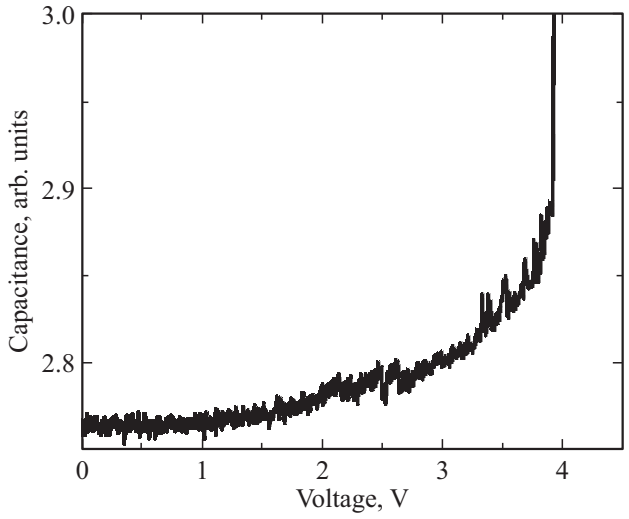


**Figure 2.** Dependence of capacitance of the contact of the AFM probe with the SZD/Pt film $C$ on voltage between the probe and the sample $U$ during electroforming.

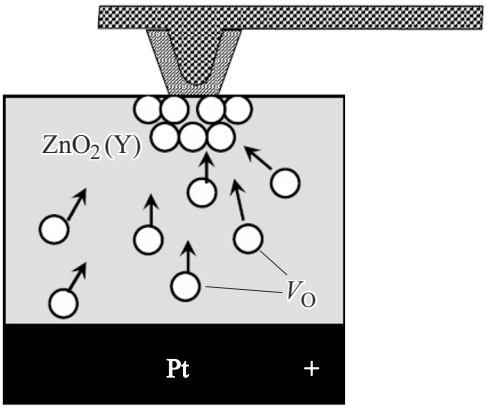


**Figure 3.** Diagram of formation of the filament of the oxygen vacancies ($V_O$) in the SZD film.

respectively, $\mu$ — mobility of the $O^{2-}$ ions in SZD, $v_{dr}$ and $F$ — a drift velocity of the oxygen vacancies and strength of the electric field in SZD in a gap between a filament extremity and the surface of the Pt sublayer. The latter can be approximately evaluated by the formula $F = U/w$, where $U$ — the difference of potentials between the AFM probe and the sample (it was assumed that the filament surface was an equipotential, whose potential was equal to the probe potential), $w = d - \ell$ — the thickness of the gap between the filament extremity and the surface of the Pt sublayer. Thus, (1) can be rewritten as

$$\frac{dw}{dt} = -\frac{n_0}{n}\frac{\mu U}{w}. \tag{2}$$

Let us assume that $U$ linearly increases with time: $U(t) = At$, where $A$ — the voltage increase rate. Then, by separating variables in (2) and integrating, we obtain

$$w^2 = -\frac{n_0}{n}\mu A t^2 + C_I. \tag{3}$$

where $C_I$ — the integration constant. For the initial conditions $w = d$ when $t = 0$, $C_I = d^2$ and

$$w(t) = \sqrt{d^2 - \frac{n_0}{n}\mu A t^2}. \tag{4}$$

Capacitance between the cylindrical filament and the Pt sublayer was evaluated using a formula for capacitance of the flat capacitor

$$C = \frac{\varepsilon\varepsilon_0 S}{w}, \tag{5}$$

where $\varepsilon$ — permittivity of SZD, $\varepsilon_0$ — the electric constant.

The area of contact of the AFM probe point with the surface of the SZD film was evaluated by solving the Hertz problem [14]. A radius of the area of contact of two elastic balls with the radii $R_1$ and $R_2$

$$R_C = \sqrt[3]{\frac{F_n R}{K}}, \tag{6}$$

where $F_n$ is a loading force, $1/R = 1/R_1 + 1/R_2$,

$$\frac{1}{K} = \frac{3}{4}\left(\frac{1-\gamma'^2}{E'} + \frac{1-\gamma^2}{E}\right), \tag{7}$$

$E$ and $E'$ — the values of the Young's modulus, $\gamma$ and $\gamma'$ — the values of the Poison's ratio for SZD and Pt, respectively. For contact of the flat sample ($R_2 = \infty$) and the AFM probe with the point curvature radius $R_p$ we have $R = R_1 = R_p$. In the experiment, the value of the loading force $F_n \sim 1$ nN, $R_p \sim 35$ nm, then we obtain $R_C \sim 5$ nm [15].

Figure 4 shows the model dependence $C(U)$ for electroforming with linear sweep of $U$ from 0 to 5 V for 5 s ($A = 1$ V/s). The parameters of the SZD film were assumed to be: $\mu \approx 4 \cdot 10^{-13}$ cm$^2$V$^{-1}$s$^{-1}$ [16], $\varepsilon = 25$, $d = 10$ nm.The concentration of the oxygen vacancies in the initial material was assumed to be equal t one vacancy per four lattice SZD cells (which corresponds on average to one Y atom per two lattice cells, which in turn corresponds to a molar portion of the stabilizing oxide $Y_2O_3$ in SZD 0.125), while inside the filament it was two oxygen vacancies per one lattice cell (which corresponds to replacing on average 1/4 of oxygen ions with the vacancies).

It should be noted that since the formula (6) does not take into account edge effects, it can be applied when $d \ll 2R_C$. Since, as shown above, in the experiment $d \sim 2R_C$, the provided calculations are of an estimated nature. Nevertheless, the model dependence $C(U)$ of Figure 4 qualitatively reproduces the dependence $C(U)$ that is experimentally measured (Figure 2).

It should be also noted that the estimated filament capacitance $C \sim 10^{-17}$ F exceeds a detection threshold of the used measurement installation, which can be considered as substantiation of traceability of the filament growth by the contact capacitance AFM method.

Besides, it should be underlined that electron transport via the filament is performed as per the hopping mechanism across the oxygen vacancies [11]. In order to measure

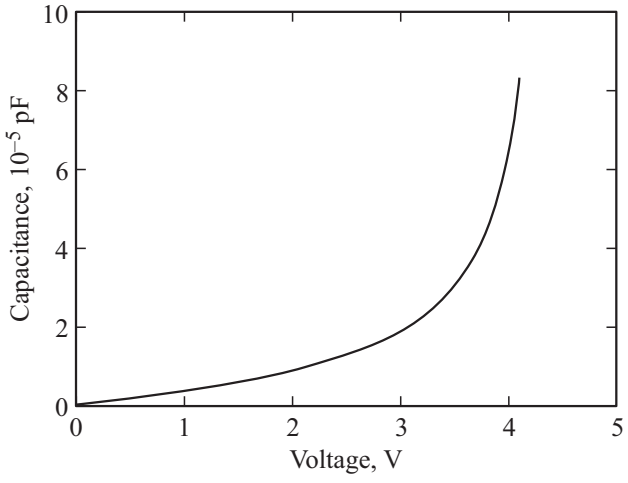


**Figure 4.** Model dependence $C(U)$ for electroforming with linear sweep of $U$ from 0 V to 5 V.

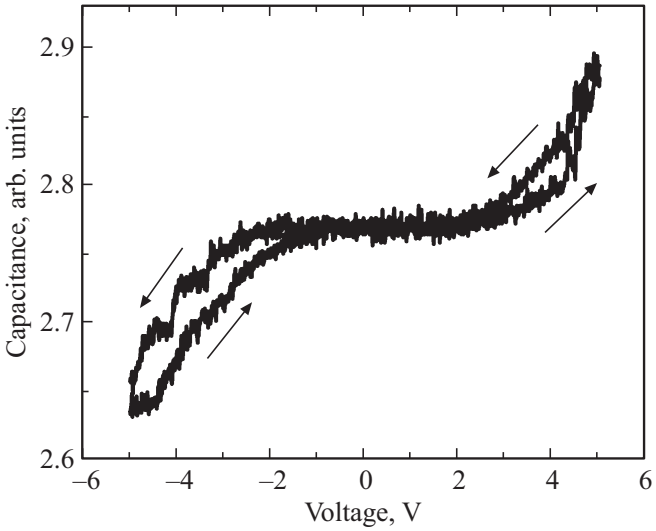


**Figure 5.** Dependence of capacitance of the contact of the AFM probe with the SZD/Pt film $C$ on voltage between the probe and the sample $U$ during cyclic switching.

the filament capacitance, it is necessary that an average frequency of electron hops between adjacent vacancies exceeds a frequency of testing variable voltage. Tunneling transparency $D$ of a potential barrier between the two oxygen vacancies that are separated by a gap of the thickness of $L$ can be evaluated in a quasi-classical approximation:

$$D \approx \exp\left(-\frac{2L}{\hbar}\sqrt{2mE_i}\right), \qquad (8)$$

where $E_i \approx 0.4\,\text{eV}$ [17] — the energy of ionization of a deep level related to the oxygen vacancy in SZD, $m \approx 0.6m_0$ — the effective mass of the electron at the conduction band bottom in SZD [18] ($m_0$ — the mass of the free electron). Probability of tunneling of the electron to the adjacent vacancy per unit time can be evaluated by the formula $\omega \approx DE_i/\hbar$. For $L = 0.4\,\text{nm}$ (which corresponds to an average distance between the oxygen vacancies in the SZD lattice when 1/4 of oxygen ions in the lattices are replaced with the vacancies) we obtain $\omega \approx 10^{13}\,\text{Hz}$, which significantly exceeds the frequency of the testing variable signal (10 MHz).

It should be also noted that the experimentally measured dependence $C(U)$ includes a constant component due to parasitic capacitance between the studied sample and the other parts of the installation. This component was neglected during simulation.

The dependence $C(U)$ that was measured during cyclic sweep of $U$ from $-5\,\text{V}$ to $5\,\text{V}$ and backwards (Figure 5) is related to variation of the filament geometry (increase and decrease of its sizes) in the electric field between the AFM probe and the Pt sublayer.

Hysteresis of the dependence $C(U)$ in Figure 5 may be related to resistive switching. It should be noted that the above-described model takes into account only the flow of the oxygen vacancies to the surface of a growing filament due to drift of the vacancies in the electric field between the AFM probe and the Pt sublayer. At the same time, it did not take into account a diffusion flow of the vacancies due to the difference of concentrations of the oxygen vacancies inside and outside the filament ($n$ and $n_0$, respectively). The more precise model of filament growth shall take into account not only the processes of drift and diffusion of the oxygen vacancies, but a real form of the filament in the dielectric film.

Figure 6 shows the AFM image of the surface microrelief and the map of distribution of capacitance along the surface of the AFM/Pt $C(x, y)$ after measurement of the dependence $C(U)$ during cyclic sweep of $U$. On the map $C(x, y)$, in the point of measurement of the dependence $C(U)$ we observed local increase of $C$, which was related to formation of the vacancy filament. The AFM image of the

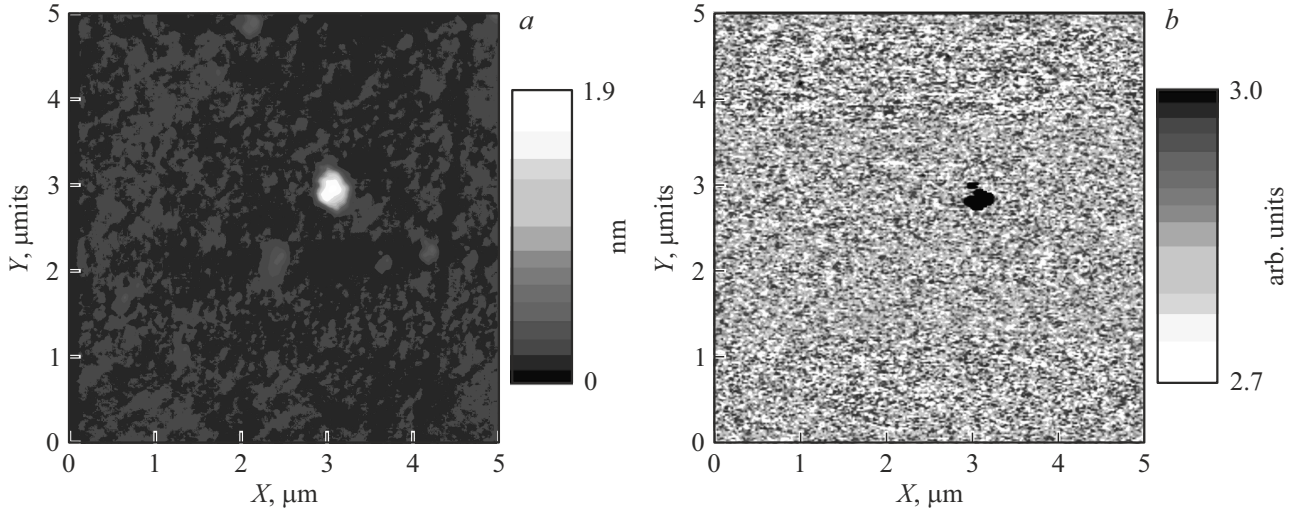


**Figure 6.** Microrelief of ($a$) and the map of capacitance distribution along the surface of ($b$) the SZD/Pt sample after measuring the dependence $C(U)$.

surface of the sample (Figure 6, *a*) exhibited local swelling of the surface of the SZD film in a location of filament formation, which was related to accumulation of the $O^{2-}$ ions under the surface of the film under effect of the electric field between the AFM probe and the Pt sublayer [15] (the end of sweep of $U$ corresponded to a positive potential of the AFM probe in relation to the Pt sublayer, i. e. the $O^{2-}$ ions were attracted to the AFM probe).

## 4. Conclusion

The results of the performed studies show that it is possible to apply the contact capacitance AFM method for tracing dynamics of variation of the geometrical size of individual conducting filaments during electroforming and cyclic switching of the virtual memristor that is the contact of the AFM probe with the surface of the oxide film on the conducting substrate, by variation of capacitance between the AFM probe and the conducting substrate using the mathematical model that relates the latter to the filament geometry. At the same time, further improvement of the mathematical mode of filament dynamics during electroforming and resistive switching is needed, which would take into account the processes of drift an diffusion of the oxygen vacancies in the oxide film as well as the real geometrical form of the filament.

### Funding

The study was performed under the State Assignment No. FSWR-2025-0006. The studies were conducted using the equipment of the Center for Collective Use of the Scientific and Educational Center „Physical of Solid-state Nanostructures“ and the Educational Design Center of Electronics of Lobachevsky State University of Nizhny Novgorod.

### Conflict of interest

The authors declare that they have no conflict of interest.

## References

[1] Y. Xiao, B. Jiang, Z. Zhang, S. Ke, Y. Jin, X. Wen, C. Ye. Sci. Technol. Adv. Mater. **24**, *1*, 2162323 (2023). DOI: 10.1080/14686996.2022.216232
[2] D. Zhu, Y. Li, W. Shen, Z. Zhou, L. Liu, X. Zhang. J. Semicond. **38**, *7*, 071002 (2017). DOI: 10.1088/1674-4926/38/7/071002
[3] J. Zhu, T. Zhang, Yu. Yang, R. Huang. Appl. Phys. Rev. **7**, *1*, 011312 (2020). DOI: 10.1063/1.5118217.
[4] F. Zahoor, T.Z.A. Zulkifli, F.A. Khanday. Nanoscale Res. Lett. **15**, *1*, 90 (2020). DOI: 10.1186/s11671-020-03299-9
[5] D. Ielmini. Semicond. Sci. Technol. **31**, *6*, 063002 (2016). DOI: 10.1088/0268-1242/31/6/063002
[6] S.H. Lee, X. Zhu, W.D. Lu. Nano Res. **13**, 1228 (2020). DOI: 10.1007/s12274-020-2616-0
[7] Y. Yang, Y. Takahashi, A. Tsurumaki-Fukuchi, M. Arita, M. Moors, M. Buckwell, A. Mehonic, A.J. Kenyon. J. Electroceramics **39**, 73 (2017). DOI: 10.1007/s10832-017-0069-y
[8] M. Lanza. Materials **7**, 2155 (2014). DOI: 10.3390/ma7032155.
[9] M.A. Ryabova, D.A. Antonov, A.V. Kruglov, I.N. Antonov, D.O. Filatov, O.N. Gorshkov. J. Phys.: Conf. Ser. **2086**, 01220 (2021). DOI: 10.1088/1742-6596/2086/1/012205
[10] C. Daniel Frisbie. In: Encyclopedia of Physical Science and Technology (3rd Edition) / Ed. R.A. Meyers. Elsevier, Amsterdam (2003). P. 469–484. DOI: 10.1016/B0-12-227410-5/00675-X
[11] E.W. Lim, R. Ismail. Electronics **4**, *3*, 586 (2015). DOI:10.3390/electronics4030586
[12] Kontaktnaya Skaniruyushchaya Emkostnaya mikroskopiya (Izmeritel'nyi vkladysh AU030). Rukovodstvo po ekspluatatsii. NT-MDT. M. (2010). 28 s.] (in Russian).
[13] D.B. Strukov, G.S. Snider, D.R. Stewart, R.S. Williams. Nat. Mater. **453**, 80 (2008). DOI: 10.1038/nature06932
[14] L.D. Landau, E.M. Lifshitz. Teoriya uprugosti, Fizmatlit, M. (2003). 269 s. (in Russian).
[15] D.O. Filatov, D.A. Antonov, O.N. Gorshkov, A.P. Kasatkin, D.A. Pavlov, V.N. Trushin, I.A. Antonov, M.E. Shenina. In: Atomic Force Microscopy (AFM): Principles, Modes of Operation and Limitations / Ed. H. Yang. Nova Science, N.Y. (2014). P. 335.
[16] S. Tikhov, O. Gorshkov, I. Antonov, A. Morozov, M. Koryazhkina, D. Filatov. Adv. Condens. Matter Phys. **8**, 2028491 (2018). DOI 10.1155/2018/2028491
[17] A. Mikhaylov, A. Belov, D. Korolev, I. Antonov, V. Kotomina, A. Kotina, E. Gryaznov, A. Sharapov, M. Koryazhkina, R. Kryukov, S. Zubkov, A. Sushkov, D. Pavlov, S. Tikhov, O. Morozov, D. Tetelbaum. Adv. Mater. Technol. **5**, *1*, 1900607 (2020). DOI: 10.1002/admt.201900607
[18] G.P. Cousland, X.Y. Cui, S. Ringer, A.E. Smith, A.P.J. Stampfl, C.M. Stampfl. J. Phys. Chem. Solids **75**, *11*, 1252 (2014). DOI: 10.1016/j.jpcs.2014.05.015

*Translated by M.Shevelev*